JOURNAL OF GUIDANCE, CONTROL, AND DYNAMICS
Vol. 16, No. 4, July–August 1993

Quantitative Feedback Theory Applied to the Design of a Rotorcraft Flight Control System

R. A. Hess* and P. J. Gorder†
University of California, Davis, Davis, California 95616

Quantitative feedback theory describes a frequency-domain technique for the design of multiple-input multiple-output control systems that meet time- or frequency-domain performance criteria when specified uncertainty exists in the linear description of the vehicle dynamics. Quantitative feedback theory is applied to the design of the longitudinal flight control system for a linear model of the AH-64 rotorcraft incorporating uncertainty. In this model, the uncertainty is assigned and is assumed to be attributable to actual uncertainty in the dynamic model and to the changes in the vehicle aerodynamic characteristics that occur near hover. The model includes an approximation to the rotor and actuator dynamics. The design example indicates the manner in which handling qualities criteria may be incorporated into the design of realistic rotorcraft control systems in which significant uncertainty exists in the vehicle model.

Nomenclature

a_i = transfer function zero, rad/s
b_i = transfer function pole, rad/s
$C,(\boldsymbol{C})$ = system single-input single-output (SISO) and multiple-input multiple-output (MIMO) output
d_{ij} = disturbance (effect of jth output on ith output)
$E,(\boldsymbol{E})$ = SISO (MIMO) error
$F,(\boldsymbol{F})$ = SISO (MIMO) prefilter
f_{ij} = element of $\boldsymbol{F}$
$G,(\boldsymbol{G})$ = SISO (MIMO) compensator
g_{ij} = element of $\boldsymbol{G}$
$\boldsymbol{I}$ = identity matrix
L = loop transmission
$P,(\boldsymbol{P})$ = SISO (MIMO) plant
$\boldsymbol{P}_0$ = nominal $\boldsymbol{P}$
$P,(\boldsymbol{P}_u)$ = SISO (MIMO) set of all possible plants
p_{ij} = element of $\boldsymbol{P}$
$\boldsymbol{Q}$ = diagonal part of $\boldsymbol{P}^{-1}$
$\boldsymbol{Q}_b$ = $\boldsymbol{P}-\boldsymbol{Q}$
q = vehicle pitch rate, rad/s
q_c = command vehicle pitch rate, rad/s
q_{ij} = element of $\boldsymbol{Q}$
$R,(\boldsymbol{R})$ = SISO (MIMO) input
r_i = element of $\boldsymbol{R}$
$T,(\boldsymbol{T})$ = SISO (MIMO) closed-loop tracking transfer function
$T_a,(\boldsymbol{T}_a)$ = SISO (MIMO) set of acceptable $\boldsymbol{T}$
t_{ij} = element of $\boldsymbol{T}$
$U,(\boldsymbol{U})$ = SISO (MIMO) control inputs
w = z body axis component of vehicle velocity, ft/s
w_c = command z body axis component of vehicle velocity, ft/s
y_{ij} = ith output (created by disturbance d_{ij})
δ_b = longitudinal cyclic input, deg
δ_c = collective input, deg
τ = time delay, s
ζ_i = ith damping ratio
ω_i = ith undamped natural frequency, rad/s

Received March 11, 1992; revision received July 2, 1992; accepted for publication Aug. 25, 1992.

*Professor, Department of Mechanical, Aeronautical, and Materials Engineering. Associate Fellow AIAA.
†Graduate Student, Department of Mechanical, Aeronautical, and Materials Engineering.

Introduction

Quantitative Feedback Theory Method

THE performance requirements for modern rotorcraft are forcing the development of high bandwidth, full-authority flight control systems. Quantitative feedback theory[1] (QFT) is a very promising technique for the design of such systems in which time- or frequency-domain performance criteria are to be satisfied when specified uncertainty exists in the linear description of the vehicle dynamics.

A very brief description of the QFT technique is in order here. The reader is referred to Refs. 1–5 for a more thorough discussion of the technique. Consider the single-input single-output (SISO) system shown in Fig. 1. QFT involves a two-degree-of-freedom design (elements G and F are obtained by the designer). The first degree of freedom is exercised in obtaining the loop transmission $L(j\omega)=G(j\omega)P(j\omega)$ so that the variation of the closed-loop frequency response over the frequency range of interest is within acceptable limits for all plants $P \in P_u$, where P_u is the set of all possible plant variations created by uncertainty. The acceptable limits are obtained from time- or frequency-domain performance specifications that are interpreted in terms of bounds on the magnitude of the closed-loop frequency response. The loop-shaping procedure is accomplished so that a realizable controller $G(j\omega)$ is obtained. Next, the second degree of freedom is exercised in obtaining the prefilter $F(j\omega)$ so that the magnitude and phase of the closed-loop frequency response lie within the prescribed limits, i.e., the closed-loop transfer function $T \in T_a$ for all $P \in P_u$.

The QFT technique can also be used for disturbance rejection, either at the plant input or output. One approaches this problem with two separate designs, then selects the loop transmission such that both are satisfied. As will be seen, disturbance rejection forms an important part of the multiple-input multiple-output (MIMO) design technique to be used herein.

Although performance robustness to structured uncertainty has been emphasized in the preceding, stability robustness is also guaranteed in the design. As an example, robust stability

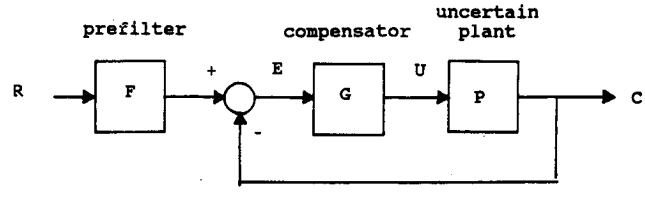

Fig. 1 SISO QFT two-degree-of-freedom problem.

can be incorporated into the design by requiring $|1+L(j\omega)| > -x$ dB at all frequencies, a requirement synonymous with keeping $L(j\omega)$ outside a circle in the complex plane centered at $-1+0j$ with a radius $\log^{-1}(-x/20)$. The specific value of x is up to the designer's discretion. Other criteria, such as limiting $|L/(1+L)|$, are also possible.

As pointed out by Horowitz,[5] the QFT method handles the problem of unstructured uncertainty, i.e., that uncertainty concerning the form or structure of the underlying plant model (typically occurring at high frequencies), by emphasizing the fastest possible decrease in $|L(j\omega)|$ with ω consistent with the satisfaction of design specifications.

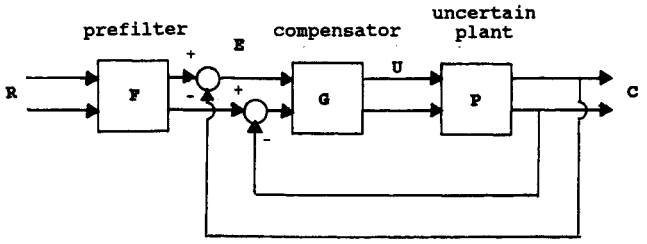

Fig. 2 MIMO QFT formulation for a 2 × 2 system.

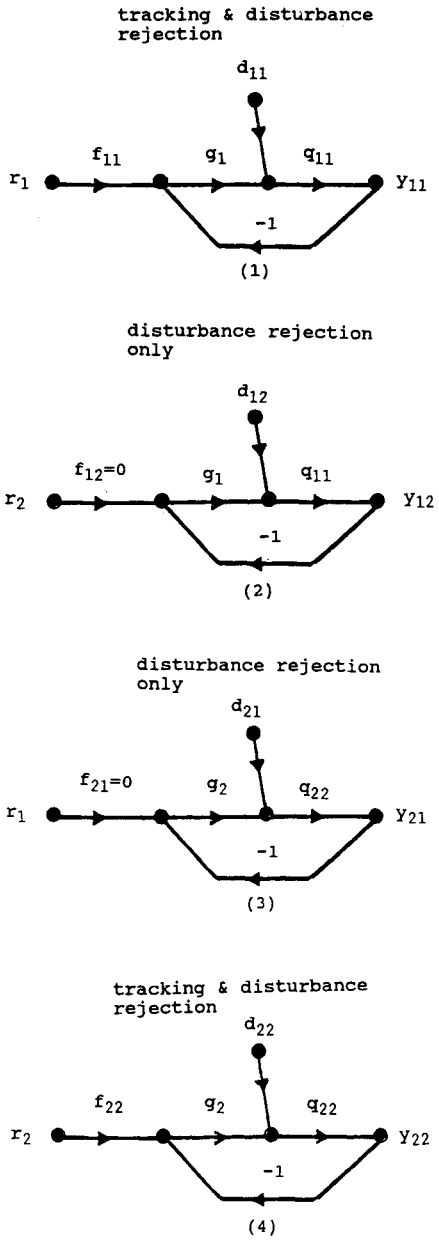

Fig. 3 MISO systems in the QFT BNIA controls approach.

QFT Design Approach for MIMO Systems

Figure 2 shows the MIMO formulation where $\boldsymbol{P}$ is now an uncertain 2×2 plant matrix, $\boldsymbol{G}$ is a 2×2 compensation matrix, and $\boldsymbol{F}$ is a 2×2 prefilter matrix. It is assumed that the determinant of $\boldsymbol{P}$ has no zeros in the right-half plane.

A number of approaches to the MIMO design exist,[5] and the method to be used herein is the so-called "basically noninteracting" (BNIA) approach. Here, one desires to minimize the off-diagonal elements of the closed-loop tracking matrix $\boldsymbol{T}$. In addition, the $\boldsymbol{G}$ matrix is assumed to be diagonal. This assumption is suited to designs in which a primary output can be associated with each control. For example, in the longitudinal helicopter control problems to be discussed, the longitudinal cyclic can be considered as a pitch-rate effector and the collective as a vertical velocity effector. The interaction or coupling that exists between controls is treated as a disturbance.

Following the treatment of Horowitz,[5] in Fig. 2, let $\boldsymbol{T}$, $\boldsymbol{P}$, $\boldsymbol{G}$, and $\boldsymbol{F}$ be 2×2 transfer function matrices with $\boldsymbol{T}=(\boldsymbol{I}+\boldsymbol{PG})^{-1}\boldsymbol{PGF}$, $(\boldsymbol{I}+\boldsymbol{PG})\boldsymbol{T}=\boldsymbol{PGF}$, and $(\boldsymbol{P}^{-1}+\boldsymbol{G})\boldsymbol{T}=\boldsymbol{GF}$. Let $\boldsymbol{P}^{-1}=\boldsymbol{Q}^{-1}+\boldsymbol{Q}_b^{-1}$, $\boldsymbol{Q}^{-1}=[1/q_{ii}]$, the diagonal part of $\boldsymbol{P}^{-1}$, and as mentioned in the preceding, let $\boldsymbol{G}$ be diagonal. Then, $\boldsymbol{Q}^{-1}(\boldsymbol{I}+\boldsymbol{QG})\boldsymbol{T}=\boldsymbol{GF}-\boldsymbol{Q}_b^{-1}\boldsymbol{T}$, and

$$\boldsymbol{T}=(\boldsymbol{I}+\boldsymbol{QG})^{-1}\boldsymbol{Q}\,[\boldsymbol{GF}-\boldsymbol{Q}_b^{-1}\boldsymbol{T}] \tag{1}$$

in which $(\boldsymbol{I}+\boldsymbol{QG})^{-1}\boldsymbol{Q}$ is diagonal. This equation yields Fig. 3, with four single-loop, multiple-input single-output (MISO) structures in which the $d_{\alpha\beta}$ are the elements of $-\boldsymbol{Q}_b^{-1}\boldsymbol{T}$. That is,

$$d_{\alpha\beta}=-\sum_{i\neq\alpha}\frac{t_{i\beta}}{q_{\alpha i}} \tag{2}$$

In Fig. 3, the r_i are unit impulses, and the interactions, or control cross couplings, have been replaced by the disturbances $d_{\alpha\beta}$. Finally, the $Y_{\alpha\beta}$ are the elements of $\boldsymbol{T}$.

The MIMO design problem is approached as follows: First, the $d_{\alpha\beta}$ are formed by replacing the right-hand side of Eq. (2) with

$$d_{\alpha\beta}\rightarrow\sum_{i\neq\alpha}\frac{|t_{i\beta}|_{\max}}{|q_{\alpha i}|_{\min}} \tag{3}$$

Here, $|t_{i\beta}|_{\max}$ represents the maximum allowable magnitude of the control cross coupling as a function of frequency and is part of the design performance specifications. Note that because relative phase information about the ratio $t_{i\beta}/q_{\alpha i}$ appearing within the summation in Eq. (2) is not available because of uncertainty, Eq. (3) has been obtained by replacing the absolute value of the sum by the sum of the absolute values, and hence a certain amount of conservatism has entered the design.

Second, the $f_{\alpha\beta}$ and g_α that guarantee that the output of each MISO system is in the acceptable set of closed-loop systems for all possible plants are selected, i.e., $\boldsymbol{T}\in\boldsymbol{T}_a$ for all $\boldsymbol{P}\in\boldsymbol{P}_u$. This selection is accomplished using the well-established MISO QFT procedure.

Schauder's fixed point theorem[5] can be used to prove that, under very general conditions, the $f_{\alpha\beta}$ and g_α just obtained solve the original MIMO uncertainty problem. These general conditions are[2] that 1) $\boldsymbol{P}^{-1}$ exists for any possible set of plant parameters and 2) for the $n=2$ cases to be studied here, as $s\rightarrow\infty$, $|p_{11}p_{22}|>|p_{12}p_{21}|$. Conditions for $n>2$ are discussed in Ref. 2.

Design Example: AH-64

Vehicle Dynamics with Uncertainty

In addition to providing a challenging QFT design problem, the AH-64 has been used in other design studies.[6-8] Rate com-

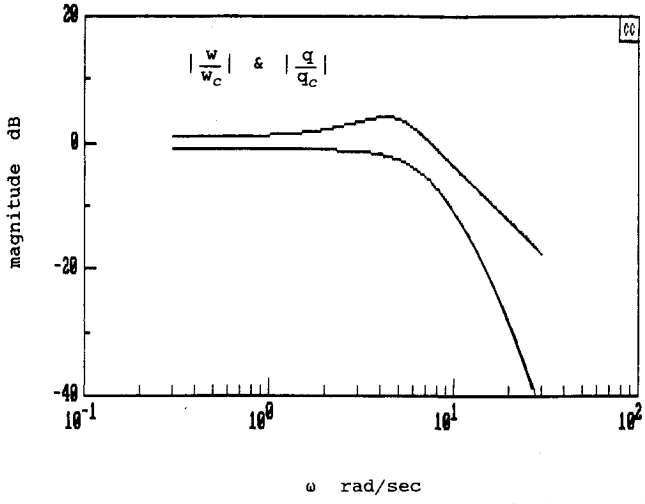

Fig. 4 Upper and lower bounds on closed-loop command/response characteristics.

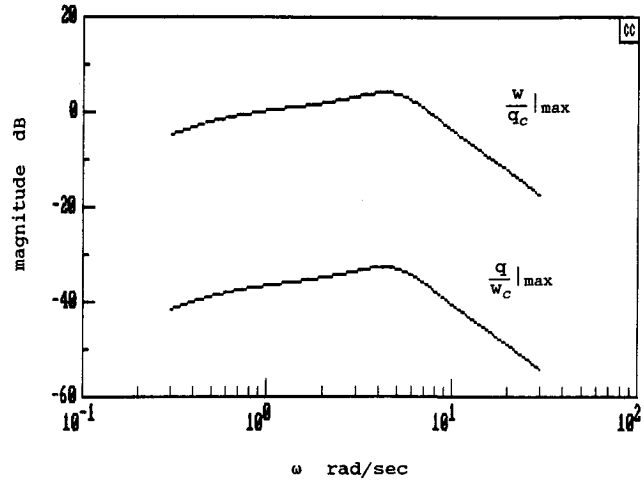

Fig. 5 Upper bounds on cross-coupling characteristics.

mand systems in both pitch and vertical translation are desired. As was discussed by Tischler, for hovering and low-speed flight, the rotor dynamics can be modeled in a manner exactly like an actuator.[9] This approach was followed by Osder and Caldwell for the AH-64,[6] and their model of vehicle, rotor, and actuator dynamics forms the basis of that used in this study.

The rigid-body longitudinal dynamics (no rotor or actuator dynamics) were obtained by the constrained variable method,[9] which includes the lateral rigid-body dynamics but assumes that infinitely tight feedback loops are used to constrain the lateral degrees of freedom. This method is more accurate than approaches in which lateral coupling terms in a six-degree-of-freedom model are simply ignored.[9] The constrained variable dynamics were obtained using "coupling numerators."[10] Next, lower-order fits to the rigid body transfer functions resulting from the constrained variable method were obtained. Finally, the rotor and actuator dynamics were appended to the rigid body transfer functions and uncertainty was assigned to the resulting gains and pole/zero combinations when expressed in Bode form (all coefficients of s^0 in the numerator and denominator are equal to unity). The resulting dynamic model, with assigned uncertainty, was treated as a veridical model of the vehicle dynamics and served as the starting point for the QFT design.

The manner in which uncertainty was incorporated in the AH-64 model was obviously artificial. This approach was necessary, because no data were available describing the variation

Table 1 Plant matrix definition with parameter variation

$p_{11}=\frac{q}{\delta_b}=\frac{K_1(0)^2e^{-\tau_1 s}}{[\zeta_1,\omega_1](b_1)(b_2)^2}$ [a]	$P_{12}=\frac{q}{\delta_c}=\frac{K_3(0)^2}{(b_5)(b_6)[\zeta_3,\omega_3][\zeta_4,\omega_4]}$
$p_{22}=\frac{w}{\delta_c}=\frac{K_2}{[\zeta_2,\omega_2](b_3)(b_4)}$	$P_{21}=\frac{w}{\delta_b}=\frac{K_4(a_1)(a_2)(a_3)e^{-\tau_2 s}}{(b_7)^2(b_8)(b_9)[\zeta_5,\omega_5]}$
$K_1\in$ [−145.6, −437.2] rad/s/deg	$K_3\in$ [210.8,285.2] rad/s/deg
$\tau_1\in$ [0.015,0.025] s (rotor)	$b_5=0.0278$ rad/s
$\zeta_1\in$ [−0.704, −0.313]	$b_6\in$ [0.725,1.09] rad/s
$\omega_1\in$ [0.460,0.690] rad/s	$\zeta_3\in$ [0.345,0.461]
$b_1\in$ [0.725,1.09] rad/s	$\omega_3\in$ [15.0,22.5] rad/s
$b_2=35.97$ rad/s (rotor/actuator)	$\zeta_4\in$ [−0.704, −0.313]
	$\omega_4\in$ [0.460,0.690] rad/s
$K_2\in$ [−81,061, −75,095] ft/s/deg	$K_4\in$ [23.9,161.8] ft/s/deg
$\zeta_2\in$ [0.345,0.461] (rotor)	$a_1\in$ [−3.76, −2.50] rad/s
$\omega_2\in$ [15.0,22.5] rad/s (rotor)	$a_2\in$ [−0.06, −0.03] rad/s
$b_3\in$ [0.253, 0.506] rad/s	$a_3\in$ [−5.81, −3.88] rad/s
$b_4=35.97$ rad/s (actuator)	$\tau_2\in$ [0.015,0.025] s
	$b_7=35.97$ rad/s
	$b_8\in$ [0.725,1.09] rad/s
	$b_9\in$ [0.253,0.506] rad/s
	$\zeta_5\in$ [−0.704, −0.313]
	$\omega_5\in$ [0.460,0.690] rad/s

[a] $(a)=(s+a)$; $[\zeta,\omega]=(s^2+2\zeta\omega s+\omega^2)$.

in vehicle dynamics with airspeed around hover, nor did the authors have enough experience to assign uncertainty to the hover dynamic model reported in Ref. 6. This study was not intended to be a rotorcraft modeling effort but rather a demonstration of the capabilities of the MIMO QFT technique in rotorcraft control problems.

Table 1 shows the variation in the elements of the plant matrix $\boldsymbol{P}$ due to the assigned uncertainty. Note the existence of unstable dynamics and an uncertain time delay in the model. The largest value of the uncertain natural frequency of the rotor dynamics (22.5 rad/s) is less than the nominal 30 rad/s value used in Ref. 6. The lower undamped natural frequencies for the rotor dynamics were assigned to provide a challenge to the design.

Desired Performance

The desired closed-loop command/response frequency domain characteristics for pitch rate and vertical translation rate are shown in Fig. 4. The lower limit was obtained by selecting "phase delay" and "bandwidth" values that just met level 1 handling qualities as reported in Ref. 11 for pitch-rate systems and then creating a simple transfer function that exhibited these phase delay and bandwidth values. The dc gain of the transfer function was then reduced to allow some performance variation at low frequency. The upper limit was obtained by modifying the lower limit transfer function to produce the bound shown in Fig. 4. The definition of the upper limit is thus somewhat arbitrary. The same performance boundaries were adopted for the vertical translation rate system. The current military specification[11] requires a "qualitative" first-order appearance in the vertical rate response following a step collective input. The minimum time constant in this first-order response is specified as 5 s. Thus, the performance bounds being enforced in Fig. 4 for the vertical rate response are very conservative.

Note that forcing both pitch and translational rate systems to have approximately the same bandwidth has been done for the purposes of exposition because it presents a challenging design problem in which significant cross-coupling effects will almost inevitably occur. Finally, it must be emphasized that the QFT technique is based on maintaining the magnitude of the system closed-loop transfer functions within desirable limits. Nothing is said about phase. Thus, it is important to ascertain whether a system that meets (or violates) the magnitude boundaries of Fig. 4 meets (or violates) the original phase delay and bandwidth specifications from which these boundaries

were created and that defined the original handling qualities specification. We shall return to this later.

The desirable cross-coupling characteristics are defined by frequency-dependent maximum allowable values for the w/q_c and q/w_c transfer functions. The subscript c refers to command variables. No guidance exists for selecting these characteristics, and the current military specification focuses on coupling between pitch and roll, heave and yaw, etc.[11] The limits selected were felt by the authors to represent reasonable characteristics, and for the purposes of this study can be assumed to represent maximum values for acceptable handling qualities. The cross-coupling boundaries are shown in Fig. 5.

QFT Design

As already outlined, the MIMO QFT design is broken down into four MISO QFT designs. It is easily determined that the two constraints on the plant matrix P are met here. Space does not permit a detailed description of the QFT design. However, Figs. 6 and 7 show the Nichols charts with the resulting loop transmissions corresponding to the first and fourth of the systems of Fig. 3. These figures correspond to the two tracking/disturbance rejection loops that were the most restrictive in the design procedure. The QFT design requires the loop

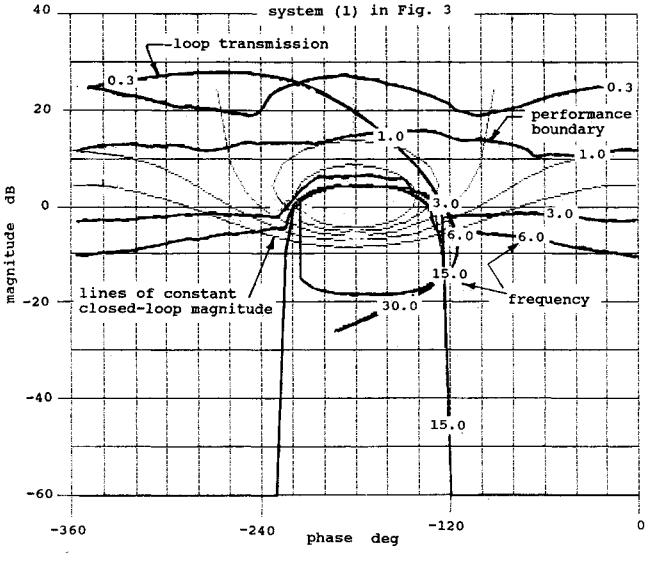

Fig. 6 Nichols chart MISO QFT design: pitch-rate loop.

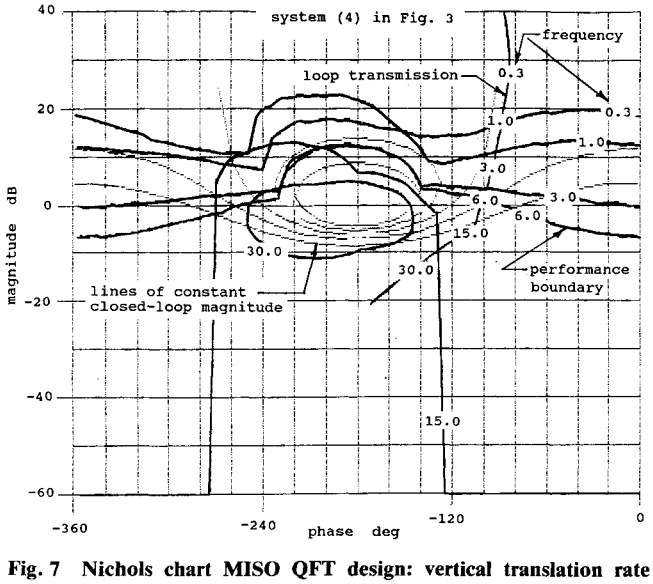

Fig. 7 Nichols chart MISO QFT design: vertical translation rate loop.

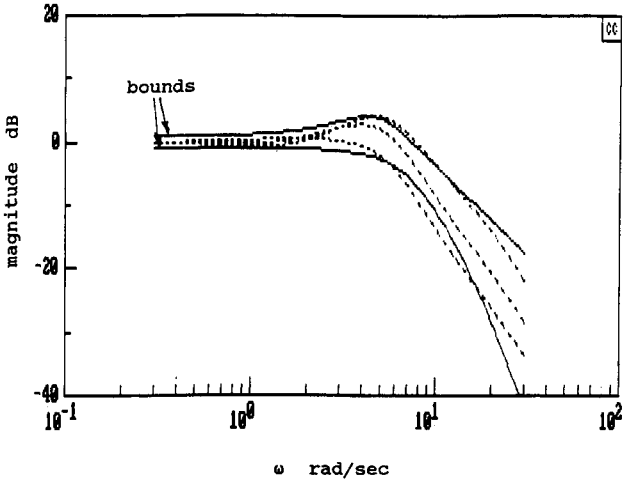

Fig. 8 Comparison of system performance with bounds: q/q_c.

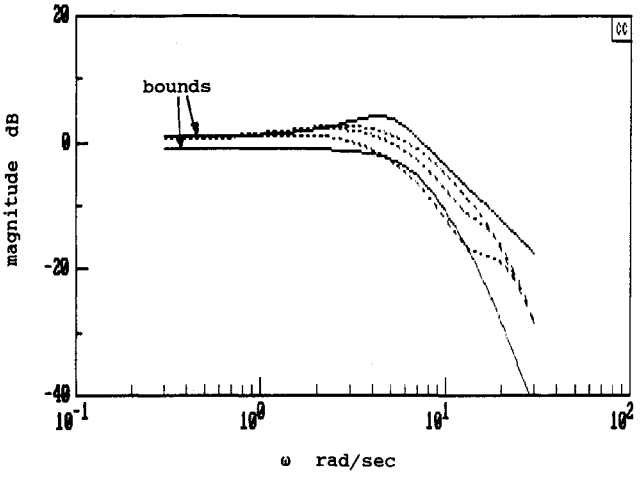

Fig. 9 Comparison of system performance with bounds: w/w_c.

transmission to lie above the appropriate boundaries shown in Figs. 6 and 7 (and the two Nichols charts not shown) at each of a discrete number of frequencies.[1] The optimum QFT design, i.e., one that involves the least amount of overdesign and guarantees the fastest possible decrease in the loop transmission with frequency (to handle unstructured uncertainty) is one in which the loop transmission lies on the appropriate boundary at each frequency.

The boundaries themselves are an amalgam of those that result from the tracking and disturbance rejection requirements. Here, disturbance rejection implies minimizing control cross coupling. Because of uncertainty, of course, any number of loop transmissions are possible with a fixed compensator. The one shown in Figs. 6 and 7 and on which the design is based is associated with P_0, where $P_0 \in P_u$. Embedding the nominal plant as part of the synthesized nominal loop transmission helps ensure a minimal order compensator.

The number of boundaries is equal to the number of frequencies selected by the designer, in this case six. The frequencies are approximately evenly distributed logarithmically and must span the range in which the variations in the boundaries are most critical. Finally, the frequencies must extend far enough so that one is certain the loop transmission does not violate stability boundaries on the Nichols chart. Here the frequency range was two decades, from 0.3–30 rad/s. The loop shaping that led to the loop transmissions of Fig. 6 was not automated but was accomplished in efficient, iterative fashion through a QFT computer-aided-design package.[12]

Table 2 QFT compensators and prefilters

$$g_1 = \frac{-114{,}938\ (0.19)\ (0.85)\ (0.4)\ (2.1)\ (19.2)}{(0)^3(1.3)\ (300)^2}\ \text{deg/rad/s}$$

$$g_2 = \frac{-107{,}730\ [0.35,\ 14.0]\ (0.2)}{(0)\ (300)^3}\ \text{deg/ft/s}$$

$$f_{11} = \frac{5.59\ (3)\ (1.26)}{[0.5,\ 5.25]\ (0.7)}$$

$$f_{22} = \frac{8003\ (1.5)}{(11)\ (2.6)\ (20)^2}$$

$$f_{12} = f_{21} = 0$$

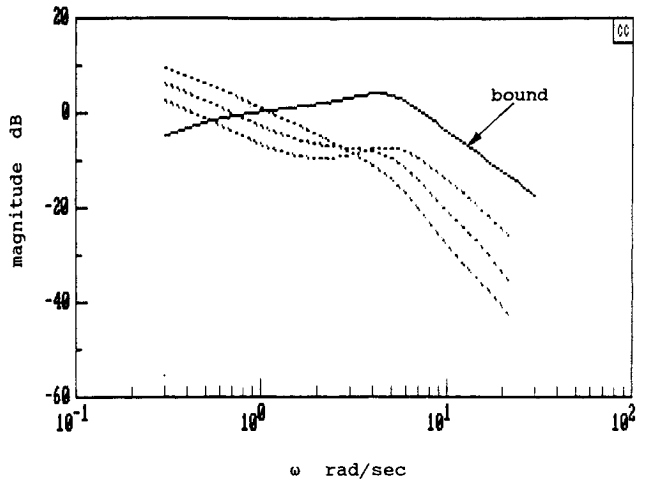

Fig. 10 Comparison of system performance with bounds: w/q_c.

Robust stability was incorporated into the design by requiring $|1+L(j\omega)| > -4$ dB at all frequencies, a requirement synonymous with keeping $L(j\omega)$ outside a 0.63 radius circle centered at $-1+0j$ in the complex plane. This requirement corresponds to gain and phase margins of 8.7 dB and 39 deg.

It should be emphasized that the QFT design summarized in Figs. 6 and 7 is certainly not an optimum one. Indeed, some violations of the frequency domain constraints are evident in Fig. 6, where the loop transmission is slightly below some boundaries. In addition, at some frequencies the design is too conservative. Of course, one may simply not be able to meet the design constraints of a specific problem when uncertainty is present. The authors are admittedly new to this game and a more seasoned QFT designer (transmission loop shaper) would likely be able to improve on this design. Table 2 shows the QFT compensators and prefilters for this design.

Figures 8–11 show the performance of the flight control systems with three sets of plant characteristics P_i selected somewhat randomly from P_u. Note that, with the exception of the low-frequency magnitudes of the w/q_c transfer functions of Fig. 12, these systems generally meet the design goals in the 0.3 to 30 rad/s frequency range used in the QFT design. An examination of the phase delay and bandwidth (as defined in Ref. 11) of the three systems here indicates that the systems do meet the original handling qualities specification. The source of the boundary violations of Fig. 10 stems from the aforementioned low-frequency loop transmission deficiencies in Fig. 6. Nevertheless, the performance violations shown in Fig. 10 are not considered a serious handling qualities problem, occurring as they do at low frequencies.

Finally, Fig. 12 shows the magnitude characteristics of the QFT compensators g_1 and g_2, listed in Table 2. The characteristics of $|g_i(j\omega)|$ determine the "cost of feedback" in terms of sensor or other system noise reflected at the plant input.[5] Specifically, $|g_i(j\omega)|$ should fall off as rapidly as possible beyond the crossover frequency ω_c to minimize noise effects. The nominal plant referred to in Fig. 12 is the one created by choosing each plant parameter to have the smallest magnitude, i.e., the first entry defining the parameter range in the bracketed pairs in Table 1. As Fig. 12 shows, the pitch-rate loop carries the highest cost of feedback in this design. The main contributor to this high cost is the uncertain time delay in the vehicle dynamics associated with longitudinal cyclic inputs.

Discussion

The design example employed here has been limited to simplified longitudinal control. This approach has been taken for the purposes of simplicity and exposition. The QFT BNIA approach can, of course, be applied to fully coupled longitudinal and lateral vehicle dynamic models. The price one would pay for this approach in terms of design complexity is that 16 rather than 4 QFT MISO designs would need to be addressed. Bear in mind that these 16 designs involve determining only 4 loop transmissions, which must not violate the boundaries of the primary command/response loops and the disturbance-only loops.

Future research will involve an examination of the flight control performance benefits of other MIMO QFT design procedures. These include 1) a sequential design approach (referred to as the fourth QFT technique in Ref. 5), wherein some

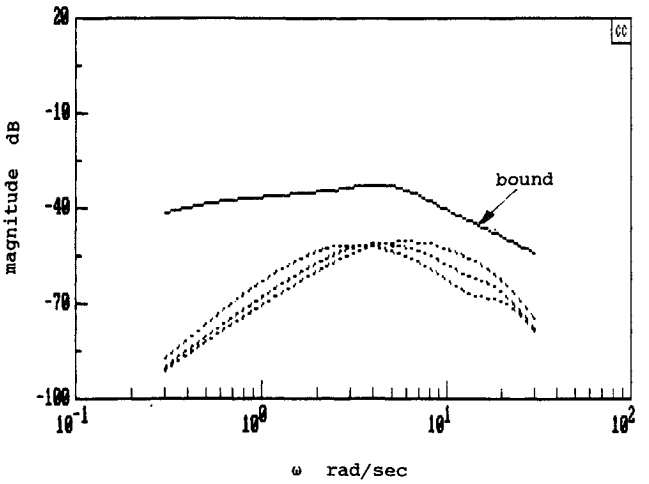

Fig. 11 Comparison of system performance with bounds: q/w_c.

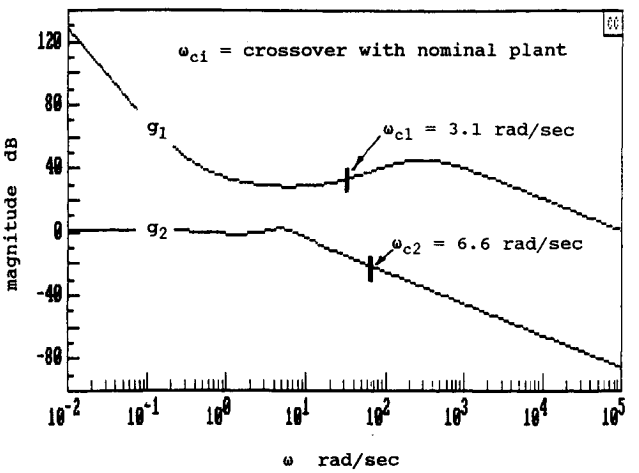

Fig. 12 QFT compensators: g_1 = pitch-rate loop, g_2 = vertical translation rate loop.

of the design conservatism in the method is removed, and 2) nondiagonal G compensation. Both of these procedures have the potential of reducing the bandwidths and cost of feedback of the diagonal loop transmissions. In addition, the simplifying assumptions employed in developing the rotorcraft models here will be eschewed to exploit the more detailed and well-documented rotorcraft models that have recently become available (see Ref. 13).

Conclusions

Based on the research described herein, the following conclusions can be made: 1) the QFT control system design methodology represents a very tractable approach to the problem of high-bandwidth rotorcraft flight control design; 2) frequency domain handling qualities criteria can be easily incorporated into the QFT design specifications; 3) the QFT diagonal compensation design was able to provide acceptable command/response performance in a challenging design example employing considerable uncertainty in the vehicle models; and 4) future work should investigate other MIMO QFT approaches and incorporate more realistic rotorcraft models.

Acknowledgments

This research was supported by NASA Grant NCC2-624, NASA Ames Research Center, Moffett Field, California. The grant technical manager is Mark B. Tischler of the Flight Dynamics and Controls Branch, whose assistance and advice are deeply appreciated.

References

[1]Horowitz, I. M., and Sidi, M., "Synthesis of Feedback Systems with Large Plant Ignorance for Prescribed Time-Domain Tolerances," *International Journal of Control,* Vol. 16, No. 2, 1972, pp. 287–309.

[2]Horowitz, I., and Loecher, C., "Design of a 3×3 Multivariable Feedback System With Large Plant Uncertainty," *International Journal of Control,* Vol. 33, No. 4, 1981, pp. 577–699.

[3]Horowitz, I., "Quantitative Feedback Theory," *IEEE Proceedings,* Vol. 129, Pt. 3, 1982, pp. 215–226.

[4]Betzold, R. W., "Multiple Input-Multiple Output Flight Control Design with Highly Uncertain Parameters; Application to the C-135 Aircraft," M.S. Thesis, Air Force Inst. of Technology, AFIT/GE/EE83D-11, Wright-Patterson AFB, OH, Dec. 1983.

[5]Horowitz, I., "Survey of Quantitative Feedback Theory (QFT)," *International Journal of Control,* Vol. 53, No. 2, 1991, pp. 255–291.

[6]Osder, S., and Caldwell, D., "Design and Robustness Issues for Highly Augmented Helicopter Controls," AIAA Paper 91-2751-CP, Aug. 1991.

[7]Garrard, W. L., Low, E., and Prouty, S., "Design of Attitude and Rate Command Systems for Helicopters Using Eigenstructure Assignment," *Journal of Guidance, Control, and Dynamics,* Vol. 12, No. 6, 1989, pp. 783–791.

[8]Ekblad, M., "Reduced Order Modeling and Controller Design for a High-Performance Helicopter," *Journal of Guidance, Control, and Dynamics,* Vol. 13, No. 3, 1990, pp. 439–449.

[9]Tischler, M. B., "Digital Control of Highly Augmented Combat Rotorcraft," NASA TM 88346, May 1987.

[10]Heffley, R. K., "A Compilation and Analysis of Helicopter Handling Qualities Data, Vol. 2: Data Analysis," NASA CR-3145, March 1979.

[11]Anon., "Aeronautical Design Standard, Handling Qualities Requirements for Military Rotorcraft," U.S. Army Aviation Systems Command, ADS-33C, St. Louis, MO, Aug. 1989.

[12]Yaniv, O., "Multiple-Input Single-Output (MISO) QFT-CAD User Manual," Dept. of Electrical Engineering-Systems, Tel-Aviv Univ., Tel-Aviv, Israel, Dec. 1991.

[13]Takahashi, M. D., "A Flight-Dynamic Helicopter Mathematical Model with a Single Flap-Lag-Torsion Main Rotor," NASA TM-102267, Feb. 1990.